Sleep Research Online 4(3): 83-90, 2001
http://www.sro.org/2001/Germain/83/

1096-214X

EEG Power Associated with Early Sleep Onset Images Differing in Sensory Content

Anne Germain* and Tore A. Nielsen**

**Département de Psychologie, **Département de Psychiatrie, Université de Montréal*
Dream and Nightmare Laboratory, Hôpital du Sacré-Coeur de Montréal, Montréal, Québec, CANADA

Relationships between known EEG changes occurring at sleep onset (SO) and processes of SO imagery formation are still poorly understood. In the present study, 24 healthy subjects signaled and reported spontaneous SO imagery while in a seated, head-unsupported position. Two judges rated the sensory content of all images. EEG samples immediately preceding the imagery signals as well as from preceding wakefulness were also recorded from a 19-channel montage. EEG samples were categorized by two judges into one of nine SO stages proposed by Hori et al. (1994). Unimodal kinesthetic images (apparent self-movement) and unimodal visual images accompanied only by SO-stage 4 were further subject to spectral analysis, topographically mapped and statistically compared. These SO images were characterized by significant decreases in all frequency bands except delta, for which significant increases were observed over several electrode sites. Kinesthetic and visual images were accompanied by different topographic patterns of delta power: kinesthetic, by prefrontal and frontal delta activation, and visual, by delta activation in more left-central and temporal regions. Results suggest that the documented spread of anterior to posterior delta power occurring for a brief window early in SO may be associated with sense-specific imagery processes unfolding over time. The results are also consistent with a novel explanation for the phenomenon of the 'sleep start' which is commonly accompanied by vivid kinesthetic images of falling at the point of sleep onset.

CURRENT CLAIM: Sleep onset images are accompanied by increased delta power, the topography of which varies from anterior to posterior sites depending upon sensory modality (kinesthetic vs. visual) of the imagery.

Early investigators observed marked changes in cognitive and physiological processes at sleep onset (SO) (Baillarger, 1845; Maury, 1848; Davis et al., 1938). Since then, researchers have documented numerous phenomenological and neurophysiological events occurring at this important transition (Kuhlo and Lehmann, 1964; Foulkes and Vogel, 1965; Vogel et al., 1966; Vogel, 1978; Richardson et al., 1981; Bosinelli et al., 1982; Cicogna et al., 1991; Cicogna, 1994; Hori et al., 1994; Lehmann et al., 1995; Michida et al., 1998, 1999; Hayashi et al., 1999). It is generally agreed that SO images are similar in many respects to dream imagery from REM sleep (e.g., hallucinatory/sensory quality, bizarreness, dynamic elements). However, as for REM sleep, there is little consensus on the precise EEG correlates accompanying SO imagery. Polysomnographic recordings have revealed 12-14 Hz EEG spindles during the SO transition (Davis et al., 1938; Dement and Kleitman, 1957; Liberson and Liberson, 1965; Hori et al., 1994) but may reflect loss of consciousness of the external environment. A diminution in the N3 ERP component may also index an attentional shift from external sensation to internal imagery (Michida et al., 1999). Occipital alpha blocking with low-voltage, 4-7 Hz theta waves has also been reported (Foulkes and Vogel, 1965; Green et al., 1970; Hori et al., 1994) that appears to be associated with high rates of imagery recall (Hayashi et al., 1987; Hori et al., 1994). EEG-derived dipoles indicate that spontaneous thoughts at SO differ in localization (anterior vs. posterior) and frequency band (delta/theta and alpha primarily) depending upon the specific content under investigation (e.g., abstract vs. visual) (Lehmann et al., 1994; Wackermann et al., 2000).

A relatively detailed scoring system employing nine EEG SO-stages has been proposed (Hori et al., 1994) that takes into consideration many of the EEG observations mentioned above (see Figure 1). These SO stages have been investigated in detail with quantitative EEG measures such as event-related potentials (ERP) (Michida et al., 1999), coherence topography (Morikawa et al., 1997; Tanaka et al., 1998, 2000), and principal-components spectral analysis (Tanaka et al., 1997). Imagery has been sampled throughout the nine SO-stages and different frequencies of recall observed for images of differing sensory modalities (Hori et al., 1994). Dream-like experiences occur most frequently in SO-stage 4 (Hayashi et al., 1999). The

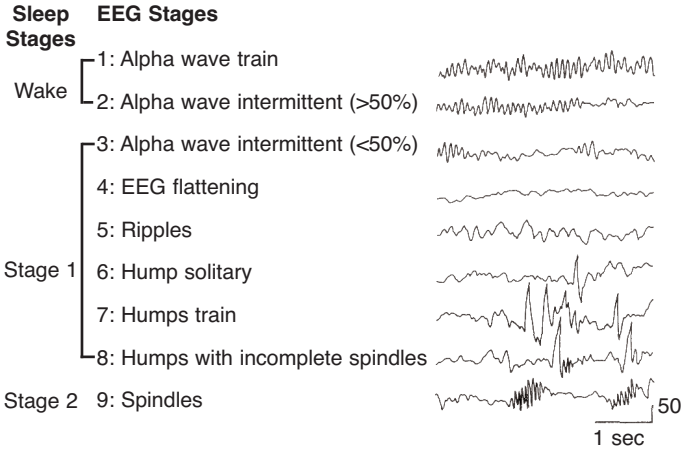

Figure 1. **Illustrations of the Nine SO Stages of the Hori et al. Sleep Onset Scoring System**. SO-stage 4, the object of the present investigation, is characterized by flattening of the EEG to less than 20 μV. (published with permission).

Correspondence: Tore A. Nielsen, Ph.D., Dream and Nightmare Laboratory, Hôpital du Sacré-Coeur de Montréal, 5400 boulevard Gouin Ouest, Montréal (Québec) Canada H4J 1C5, Tel: 514-338-2693, Fax: 514-338-2531, E-mail: t-nielsen@crhsc.umontreal.ca.

frequency of kinesthetic images peaks in SO-stage 1 then decreases steadily in later stages, whereas the opposite is true for visual images (Hori et al., 1994; Hayashi et al., 1999). However, more detailed study of SO imagery processes in relation to EEG microstructure is lacking.

In sum, it is still uncertain whether EEG changes at SO are reliable, isomorphic correlates of SO imagery. Often in SO studies, imagery is not sampled in such a way that its temporal association with SO EEG can be established with any certainty. For example, since the nine SO-stages of Hori et al. occur so close in time, the imagery reported after experimental prompting from any given stage very likely reflect processes active in any preceding stages. Further, since imagery content is typically not studied as an independent variable in SO studies (although cf. Wackermann et al., 2000), links between imagery content and specific EEG properties remain unspecified.

Our strategy has been to examine extremely brief SO images that vary in sensory content (visual vs. kinesthetic) in conjunction with microstructural attributes of the SO EEG. This approach allows us to assess both fast- and slow-changing EEG attributes in relation to specific imagery qualities.

METHODS

Subjects

Fifteen men and nine women, aged 18 to 47 years (M=25.13±6.75 yrs), each slept for two consecutive nights in the laboratory. They were healthy and suffered from no psychiatric, neurologic or sleep disorders. None reported taking medications. They were asked to abstain from ingesting alcohol, caffeine or other drugs for 24 h prior to participating. They gave informed consent to a protocol that was approved by the Hospital Ethics Committee, and were paid a small amount for participation.

Sampling of EEG Associated with SO Imagery

Prior to lights-out on each night, subjects underwent a 30-min SO imagery acquisition session. They were instructed to attempt to fall asleep while sitting upright in bed with the head unsupported and simultaneously monitoring their own thoughts. They were to detect and report any 'image, feeling, sound or thought' that they did not voluntarily produce and that seemed to be associated with the subjective feeling of falling asleep. Participants held a button switch in the right hand and used it to signal the occurrence of any such imagery. We have demonstrated with untrained participants that this procedure can be used to elicit several spontaneous SO images in a single sitting (Nielsen et al., 1995; Germain and Nielsen, 1996).

Subjects' descriptions of individual images were tape-recorded and scored by two independent judges for whether they contained unambiguous references to visual (V), auditory (A), or kinesthetic (K) sensory modalities. Kinesthetic imagery was defined as instances of apparent self-movement. These ratings were used to classify each sample as either unimodal (single sense), bimodal (two senses) or multimodal (three senses) to classify its modality type (V, A, K, VA, VK, AK, AVK) and to compare grouped frequencies with available norms (Hori et al., 1994). Interrater reliability was calculated as percent of concordance of ratings prior to attempting consensus between judges.

Each subject was fitted with a standard montage of electrodes for recording sleep (EEG, EOG, EMG, respiration, heart rate), as well as a 19-channel, 10-20 montage for EEG mapping which is described below. Subjects' signals during the imagery acquisition task triggered an acquisition program (Stellate Système Enr., 1995) that sampled the EEG and other physiological variables for a window 45 sec before and 15 sec after the signal (see Figure 2). EEG samples were digitized at 512 Hz from a 19-channel referential montage (Fp1, Fp2, F3, F4, F7, F8, C3, C4, P3, P4, O1, O2, T3, T4, T5, T6, Fz, Cz, Pz) with a common reference (A1+A2, 10 K-ohm resistance). From this montage, a whole scalp-average reference was calculated offline and applied to each channel. This montage is less susceptible to artifacts (Pivik et al., 1993). It subtracts activity that is common to a large number of electrodes, thus attenuating very widespread differences. Differences observed with the montage thus reflect changes above and beyond those common to a large number of leads. EEG signals were sampled by a Grass model 12 acquisition system (cut-offs: 0.10-100 Hz), digitally filtered with a Hanning window (a filter of cosine type which minimizes artifactual leakage), and archived on optical disk. The 512 Hz sampling frequency allowed a spectral resolution of 1 Hz for the 0-30 Hz spectrum and allowed EEG sections of as short as one second in duration to be selected for spectral analysis.

EEG tracings for each signaled image were examined independently by two experienced polysomnographers. Four consecutive 1-sec, artifact-free epochs were selected from the 10 sec of activity falling prior to the subject's signal; to avoid activity associated with the button press itself, one second of activity immediately preceding it was excluded (see Figure 2). The epoch size of 4 sec was selected to permit selection of very brief EEG epochs but also to retain compatibility with FFT analyses at other spectral resolutions, especially 128 Hz, which

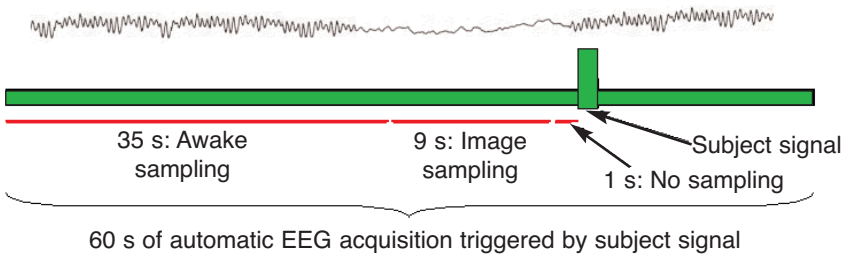

Figure 2. **Schematic Representation of the Procedure for Selecting EEG Sections for Image and Awake Samples.** EEG sampling from 35 sec of awake and 10 sec of SO-stage 4 is depicted. See text for details.

requires a minimum 4-sec epoch size with our FFT analysis software. The selected epochs were categorized into one of the nine SO-stages of the Hori et al. (1994) system. The SO-stages are defined by varying proportions of alpha activity (Stages 1, 2, and 3), by 'flattening' of waves to less than 20 μV (Stage 4), by presence of theta ripples (Stage 5), by proportions of vertex waves (Stages 6 and 7) and by the presence of spindles (Stages 8 and 9). Figure 1 illustrates these stages. EEG derivation C3 (and C4 if needed) was used to determine SO-stage. EEG samples for which raters disagreed were reviewed by both raters together and a consensus attempted. When they could not reach consensus, the image and its corresponding EEG were excluded from further analyses. Interrater reliability was calculated as percent of concordance of ratings prior to this consensus procedure.

When a subject reported more than one image with the same sensory attributes, an average of the EEG values associated with those images was calculated for that subject. Since this procedure considerably reduced the number of total images within each modality category, only the V and K categories contained enough images for statistical comparisons of EEG power and were retained for these analyses.

Each EEG sample for a signaled image was paired with an EEG sample of wakefulness that immediately preceded it. For this, four 4-sec, artifact-free samples of awake EEG were selected from the first 35 sec of the 45-sec window preceding each signaled image (Figure 2). Excluding the 10 pre-signal sec in this manner minimized potential overlap between the EEG activity presumably accompanying an image and that accompanying prior wakefulness. Wakefulness was defined as continuous alpha activity in all EEG derivations and high EMG activity in the chin EMG. The four awake EEG epochs were averaged and subjected to spectral analysis, as described below.

Three types of statistical comparisons are made possible by this design: 1) comparisons between imagery and awake EEG samples allows for detection of relatively fast EEG changes accompanying the imagery; 2) comparisons between imagery samples of different sensory modalities (kinesthetic vs. visual) allows for detection of EEG activities differentially characterizing the two imagery types; and 3) comparisons between awake EEG samples for imagery sections of different sensory modalities allows for detection of relatively slow EEG changes unique to the two imagery types that might be underway during the awake state.

For each EEG selection (image or awake), Fast Fourier transforms were computed on successive 1-sec epochs using a spectral resolution of 1 Hz. Periodograms for these computations were averaged to obtain absolute amplitude power spectra. The spectra were integrated into the following frequency bands: delta: 3-4 Hz; theta: 5-7 Hz; alpha: 8-13 Hz; beta1: 14-20 Hz; beta2: 21-30 Hz; total: 3-30 Hz.

Statistical Analyses

EEG results were examined using 2x2x19 MANOVAs with modality (visual vs. kinesthetic) as an independent variable, state (image vs. awake), and electrode site (19 leads) as repeated-measure variables, and absolute EEG power values as dependent variables in five separate analyses (delta, theta, alpha, beta1, beta2). To compensate for violations of the sphericity assumption in repeated measures, degrees of freedom were reduced by the Greenhouse-Geisser and Huynh-Feldt (H-F) corrections. Note, however, that because these assumptions are inevitably violated when multiple electrode sites reflect similar levels of activation, interaction effects are often diminished if not eliminated in such designs. Therefore, the topographic distributions of EEG power were examined *post-hoc* with *t*-tests for both state x electrode site and modality x electrode site interactions, as described below.

Topographic Statistical Mapping

Spectral scores for a given condition (imagery vs. awake or visual vs. kinesthetic) were compared using mean maps (M-maps) (Duffy et al., 1981). In the present case, these consist of color representations of average spectral amplitude power (in μV^2) for 19 original data points with quadratic interpolation of all other points. M-maps were compared statistically using paired *t*-tests for interactions involving the repeated measures factor state and independent *t*-tests with unequal variance assumptions for the independent variable modality. Results of these tests were graphically represented with probability- or *p*-maps. The latter are similar to M-maps except that the raw data before interpolation consists of *p*-values from the 19 paired *t*-test comparisons.

Hypotheses

We predicted that 1) imagery samples would have lower absolute EEG power than awake samples (i.e., significant effects involving state); 2) visual imagery samples would differ from kinesthetic samples (i.e., significant effects involving modality); and 3) these power differences would vary topographically (i.e., significant effects involving electrode site) for different imagery types. Because we limited our choice of EEG samples to SO-stage 4 (EEG flattening), we expected decreases in fast frequency bands (alpha, beta1, beta2, but especially alpha) regardless of imagery type, but differentiation of imagery type by slower frequency bands (delta, theta). Because of previous research demonstrating changes in delta power in frontal regions at sleep onset (Morikawa et al., 1997; Tanaka et al., 2000), we also expected that increases in slow frequency power would be more evident for frontal regions.

RESULTS

Subjects signaled a total of 136 images. Ten images were excluded from analysis because artifacts were present in the associated EEG samples. Raters selected the same SO EEG stage for 80.2% of the images; after consultation, six samples could not be agreed upon and were excluded from further analysis. Thus, a total of 120 images with accompanying EEG were available for spectral analysis. The number of images per subject varied between one and 12 (M=5.67, SD=3.69). The mean number of images signaled by women (M=5.67, SD=4.97) was not different from that reported by men (M=5.67, SD=2.87) (t_{22}=0.00, p=1.00).

Distribution of Modalities Over SO Stages

Of the 120 images, 80.9% (97) were classified as occurring in SO-stage 4 (EEG flattening) whereas 12.5% (15) were classified as occurring in SO-stage 5 (theta ripples). Only seven images (5.8%) occurred in SO-stages 1 or 2, a single image (0.8%) occurred in SO-stage 7, and no images occurred in SO-stages 8 and 9.

Sensory Content of Hypnagogic Images

Raters agreed on 87% of ratings of image modality; consensus could be reached for the remainder. The distribution of imagery sensory modalities appears in Table 1. Most images, 64.2%, were unimodal, consisting of either visual, auditory, or kinesthetic features alone. Another 35.0% were bimodal, consisting of some combination of two modalities. Only one image was multimodal, containing all three sense modalities. When images were unimodal, 57.1% (44/77) were visual in nature; when they were bimodal, 92.9% (39/42) were visual. For all 120 images considered together, 70.0% contained visual sensory features.

Because most SO images (80.9%) fell into SO-stage 4, we were able to select EEG samples that were uniquely characterized by this common EEG classification and, within this subgroup, compare the power spectra of images with qualitatively different sensory attributes. Of the 97 images scored as SO-stage 4, most were visual (N=38), auditory and visual combined (N=20), or kinesthetic (N=20). The others were kinesthetic and visual combined (N=11), auditory (N=6), auditory and kinesthetic combined (N=1), or all three modalities combined (N=1). We chose the two simplest, most distinct and most numerous image types, i.e., unimodal visual (N=16 subjects) and unimodal kinesthetic (N=10 subjects), for further statistical assessment of EEG correlates.

Table 1
Categorization of SO Images by Sensory Modality

Modality	N	%	%V only
V	44	36.7	36.7
K	23	19.2	
A	10	8.3	
AV	22	18.3	18.3
KV	17	14.2	14.2
KA	3	2.5	
AKV	1	0.8	0.8
Total	**120**	**100.0**	**70.0**

V=visual; K=kinesthetic; A=auditory.

Spectral Power of Kinesthetic and Visual Images

Significant main effects for both state and electrode site were observed for spectral power in all frequency bands except delta. These effects indicated that 1) awake EEG samples, for frequencies faster than delta, had higher power than did corresponding image samples–regardless of whether these were kinesthetic or visual samples; 2) image samples had higher delta power than awake samples; and 3) EEG power varied significantly according to electrode site, regardless of other conditions. There were no three-way interactions for any of the frequency bands, indicating that different configurations of EEG topography for visual and kinesthetic images could not be demonstrated for awake and image samples. However, significant state x electrode site and modality x electrode site interactions were observed for several frequency bands and are described in greater detail below.

State x electrode site interactions were observed for total, theta, alpha and beta2 (all $p<0.05$), with a trend for beta1 ($p<0.07$; see Table 2). In each case, a subset of electrodes

Table 2
State X Electrode Site Interactions for EEG Power in All Frequency Bands

	State x Electrode Site ($F_{1,18}$)[a]	Electrode Sites Affected [b]	By Modality	Electrode Sites Affected [c]	Effect[d]
Delta	0.68, p=0.69	(Fp1), Fp2, F3, F7, F8, C3, Cz, P3, (T4), T5	Kin: Vis:	Fp1, Fp2, F3, Fz, F8, (C3), (T3) F7, C3, Cz, T3, T5, T6	I>A I>A
Theta	3.02, p=0.01	Fp1, F3, Fz, F4, F7, C3, C4, P3, P4, O1, O2, T3, T4, T5, T6	Kin: Vis:	(T6) Fp1, F3, Fz, (F4), F7, C3, (C4), P4, (O1), O2, T3, (T4), T6	A>I A>I
Alpha	2.94, p=0.04	Fp1, Fp2, F3, Fz, F4, F7, F8, C3, Cz, C4, P3, Pz, P4, O1, O2, T3, T4, T5, T6	Kin: Vis:	C3, Cz, P3, (Pz), T3 Fp1, Fp2, F3, Fz, F4, F7, F8, C3, (Cz), C4, P3, Pz, P4, O1, O2, T3, T4, T6	A>I A>I
Beta1	1.92, p=0.07	Fp1, F3, Fz, F7, F8, C3, Cz, C4, P3, Pz, P4, O1, O2, T5, T6	Kin: Vis:	(F3), F7, C3, P3, Cz, Pz, T3 F7, F8, C4, P3, Pz, P4, T4	A>I A>I
Beta2	1.99, p=0.03	F7, C3, Cz, C4, P3, P4, Pz, (O1), O2, T4	Kin: Vis:	Fp2, C3, C4, P4, O2 F7, (F8), C3, P3, (Pz), T3, T4	A>I A>I
Total	2.77, p=0.03	(Fp1), F3, Fz, (F4), F7, C3, Cz, C4, P3, Pz, P4, O1, O2, T3, T4, T6	Kin: Vis:	C3 Fp1, F3, Fz, F7, C3, C4, P3, P4, O2, (T3), T4, T6	A>I A>I

[a]*H-F* adjusted df=1,3; [b]All $p<0.05$ (trends in brackets: $p<0.08$); [c]All $p<0.05$ (trends in brackets: $p<0.07$); [d]A=awake, I=imagery.

indicated reduced power during image samples regardless of whether these were visual or kinesthetic. The effect was by far most generalized for alpha, for which all 19 electrodes significantly discriminated awake from imagery samples. Next most generalized were theta and beta1, each with 15 of 19 electrodes distinguishing the samples, then beta2, with 10 of 19 electrodes. The interaction was not significant for delta, but eight electrodes discriminated between awake and image samples; for all eight, image samples had higher delta power than did awake samples. These imagery-awake differences were all examined separately for visual and kinesthetic samples as shown in the M- and *p*-maps in Figure 3.

Delta power distinguished kinesthetic from visual image samples relative to awake samples. Kinesthetic images were characterized primarily by significant increases in frontal delta power (Fp1, Fp2, F3, Fz, F8), whereas visual images were characterized by significant increases in a wider disperson of left central and temporal leads (F7, C3, Cz, T3, T5) and a single right hemisphere lead (T6) (see Figure 3, Delta). The selective association of frontal and prefrontal leads to kinesthetic imagery was further supported by *t*-test comparisons between kinesthetic and visual imagery samples (Figure 4, Delta-Image). Kinesthetic images had significantly higher delta power in Fp1, Fp2 and Fz (all $p<0.05$) than did

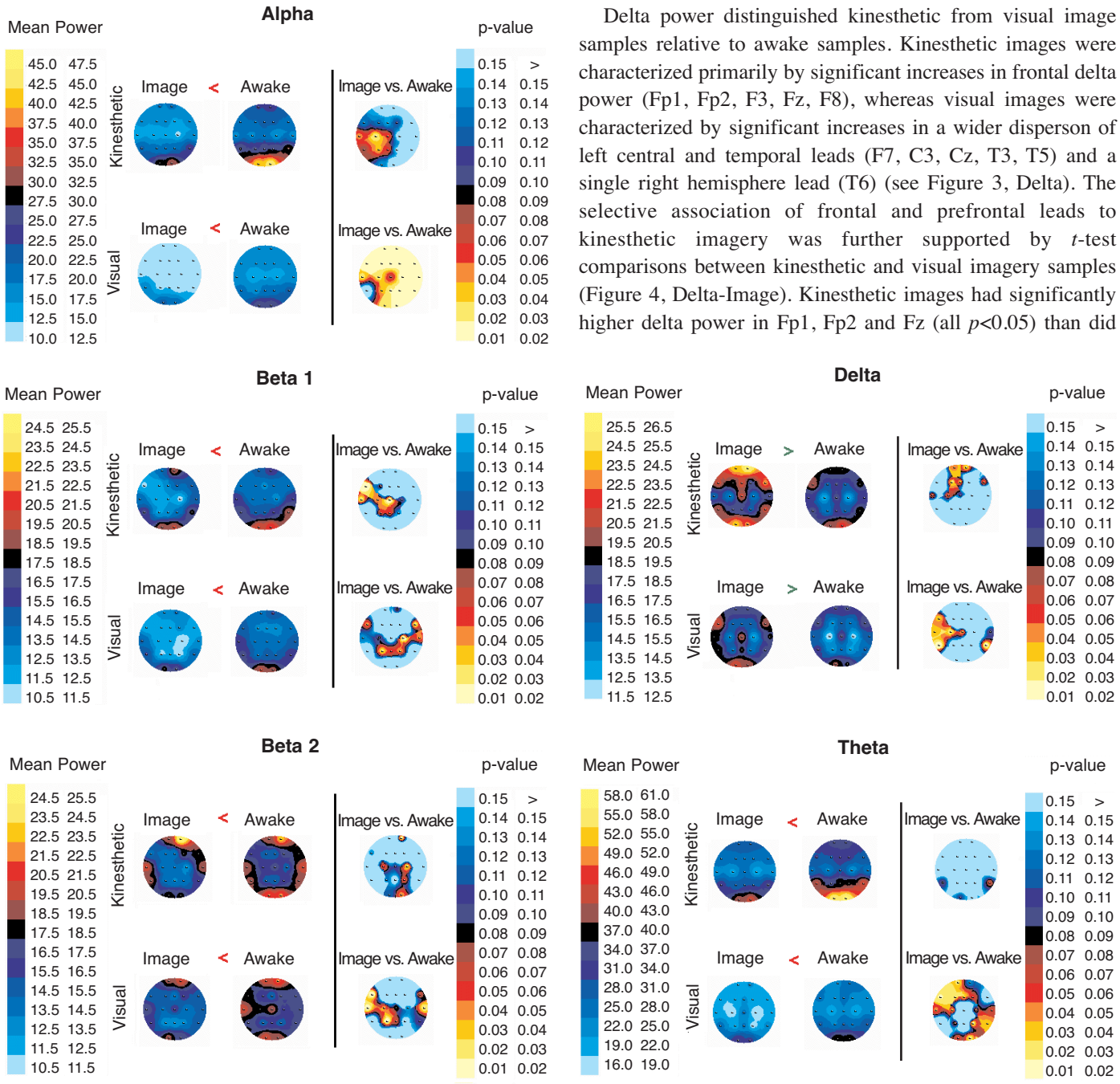

Figure 3. **Delta, Theta, Alpha, Beta1 and Beta2 Power for EEG Sections Sampled During SO Imagery (Image) and Preceding Wakefulness (Awake) for Kinesthetic and Visual Imagery Types.** Mean- or M-maps on the left of the black vertical bar illustrate mean absolute amplitude power (in μV^2) for EEG sections in each of five frequency bands. *P*-maps on the right of the vertical bar illustrate *p*-values for *t*-test comparisons between the pair of M-maps on the left: image vs. awake comparisons for both kinesthetic and visual images. On the M-maps, regions of high power are shown in yellow, orange and red hues while regions of lower power are shown in black and blue. On the *p*-maps, regions that statistically differentiate the two EEG samples are shown in yellow, orange and red while regions that do not are shown in darker hues. M-map scales may differ for the different frequency bands; *p*-map scales are constant for all bands. Delta power for image sections increased (>) in several electrode sites compared with awake sections for both kinesthetic and visual samples. Power in theta, alpha, beta1 and beta2 bands decreased (<). Decreases were most generalized for alpha.

visual images; trends were observed for F3 and T3 (all $p<0.11$). There were no differences observed for the awake state comparisons between these two conditions (Figure 4, Delta-Awake).

Increased alpha power also distinguished kinesthetic from visual images, although the topographic profiles were somewhat different. This effect is less easy to appreciate in the maps in Figure 3 (Alpha-Image) because of the widespread diminution of alpha power for visual images relative to awake. However, *t*-test comparisons between kinesthetic and visual imagery samples revealed less diminution of alpha power for kinesthetic than for visual samples (Figure 4, Alpha-Image). Kinesthetic images had higher alpha power in prefrontal (Fp1, Fp2) and right temporal-parietal (T6, P4) sites than did visual images; trends were observed for F8, T4, and O2 (all $p<0.10$). Again, there were no differences observed for awake state comparisons between these two conditions (Figure 4, Alpha-Awake).

No other frequency bands differentiated kinesthetic from visual images with clear topographic patterns. It is noteworthy, however, that the two types of imagery were differentiated by only a single frontal electrode site for each of the remaining frequencies; these were Fp1 for theta power and Fp2 for both beta1 and beta2 power (all $p<0.05$). Power was greater for kinesthetic than for visual images in each case. No differences between awake samples was observed for any of these frequencies.

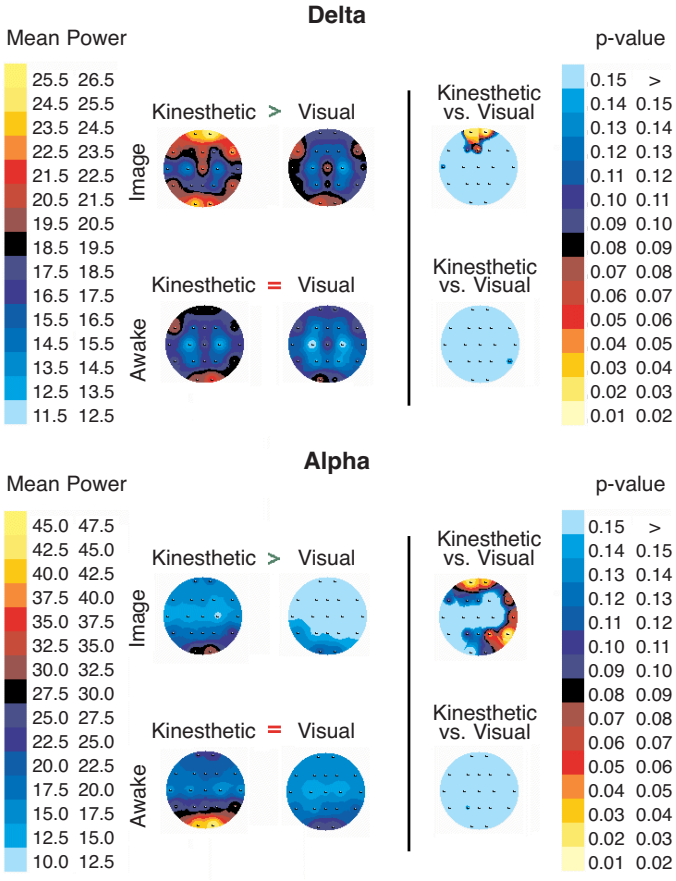

Figure 4. **Delta and Alpha Power for EEG Sections Sampled During Kinesthetic and Visual SO Images.** *P*-maps illustrate *p*-values for *t*-test comparisons between the pairs of M-maps on the left: kinesthetic vs. visual comparisons for both image and awake samples. Legends as in Figure 3. Delta power is greater for kinesthetic than for visual images over prefrontal and frontal electrode sites; awake samples do not differ. Alpha power is also greater for kinesthetic than for visual images over prefrontal sites and a wider distribution of lateral right hemisphere sites. Awake samples again do not differ.

DISCUSSION

The high proportion of images that we observed in SO-stage 4 and, to a lesser extent, SO-stage 5 seems at first inconsistent with the finding that SO-stage 4 occupies only 5.1% (0.9 min) of the total sleep onset interval, that 13% of subjects appear to lack this stage altogether (Tanaka et al., 1996), and that probed recall of imagery in this stage is only 37.7% (Hori et al., 1994). However, it is likely that our imagery acquisition method (subjects seated with head unsupported) was responsible for the preponderance of awakenings in this early SO stage. Findings from two previous self-observational studies (Nielsen, 1991, 1995) suggested that images produced with this method are temporally-linked to the initiation of muscle atonia and/or phasic neuromuscular events such as limb twitches and head jerks. If this is the case, then it is also likely that atonia-linked movements experienced by our subjects during the task awakened them before they progressed beyond SO-stage 4 or, at most, 5. This possibility could explain not only the preponderance in our sample of images in SO-stage 4, but also the fact that these images were preponderantly very simple, characterized by only a single sensory modality. Note that Hori et al. (1994) reported that all SO images from all nine categories were unimodal in nature. Our finding that bi- and multi-modal images are quite common (35.8%), even in early SO-stages 4 and 5, suggests that Hori et al. likely categorized their images according to their predominant sense modality, perhaps to avoid the problem inherent in scoring and classifying various bimodal combinations (AV, KV, KA, etc).

Our topographic analyses also support the notion that the SO images were products of an interruption early in the imagery generation sequence and, further, they link together two previous findings in a way that clarifies the nature of this sequence. These two findings are that 1) delta power increases dramatically during SO, an increase first evident in frontal regions, and 2) kinesthetic imagery is more frequent than visual imagery early in SO. These findings are described in more detail below.

In the present results, delta power in several electrode sites was alone in increasing during SO imagery, whereas power in all other frequency bands decreased. It is well-established that the first three minutes of SO is characterized by a dramatic increase in delta power relative to other frequency bands (Ogilvie et al., 1991; Merica and Gaillard, 1992; Morikawa et al., 1997). Initially, this change in Delta activity is localized to frontal cortex and subsequently spreads to central, parietal and temporal cortex (Morikawa et al., 1997), building in both

amplitude and coherence (Tanaka et al., 2000). The abruptness of this increase may reflect the sudden activation of brief SO imagery processes. A PET investigation demonstrated that increases in delta power early in sleep are positively correlated with regional cerebral blood flow, a finding which may mean that delta power, in fact, indexes mentation occurring in NREM sleep (Hofle et al., 1997).

Changes in delta power topography were markedly different for kinesthetic and visual images in the present results. It has been shown previously that the frequency of kinesthetic images ('bodily imagery') during SO attains its peak in SO-stage 1 then decreases in subsequent stages, whereas the opposite is true for visual images (Hori et al., 1994; Hayashi et al., 1999). Thus, it may be that the kinesthetic and visual images assessed in our study also differed in the temporal order in which they appeared in the SO interval. Kinesthetic images, which we found to be linked to frontal delta power, likely occurred early in the imagery generation sequence, because delta power is predominant in frontal regions very early in SO. Visual images, linked with left-side posterior regions, may have occurred later in the sequence, when delta power changes have been observed to spread to more lateral, posterior, and largely left-hemisphere sites.

This conceptualization of a temporally-organized SO image formation sequence is supported by our finding that alpha power was higher for kinesthetic than for visual images; higher alpha suggests that the EEG may have been sampled from earlier in SO-stage 4 when wave 'flattening' was less complete. This conceptualization is also consistent with evidence that prefrontal cortex is implicated in creating dynamic motor images and maintaining them in working memory (Decety, 1996), whereas more posterior areas, e.g., visual association cortex, are implicated in REM sleep when visual imagery is most intense (Braun et al., 1997). Some (Bertini and Violani, 1984; Greenberg and Farah, 1986; Antrobus, 1987), but not all (Solms, 1997), authors also link dream imagery to primarily left-hemisphere activity, which corresponds to the present finding of a predominantly left-hemisphere activation in delta power during visual imagery.

The proposed description of an imagery generation sequence may help to explain the commonly observed phenomenon of 'sleep starts' or 'hypnic jerks' that involve compelling kinesthetic images such as falling or stepping off into space. The fact that such episodes appear to occur precisely at sleep onset may reflect the activation of exclusively kinesthetic imagery associated with highly localized, prefrontal delta activity early in SO, as proposed above. Such a model of SO imagery may also have implications for theories that consider visual dreams to be based upon kinesthetic images (Lerner, 1967; Newton, 1970).

The present findings should be qualified in some respects. First, sample sizes could be larger for topographical analyses with multiple frequency bands. Second, dreams rather than subjects were used as units of analysis for the descriptive statistics dealing with imagery frequency and quality; these results may have been biased in favor of those subjects reporting several images. Third, it is possible that because we sampled the EEG with epoch lengths that were slightly shorter (4 sec) than those used by Tanaka, et al. (1996) (5 sec), we identified slightly more Stage 4 reports than did the latter authors. In contrast, it should be noted that the 4-sec epoch affords more precision in identifying brief EEG changes than does the 5-sec epoch. Fourth, it might be argued that the EEG differences that we observed between visual and kinesthetic images are due to sensorimotor processes associated with execution of the button press rather than to imagery processes *per se*. However, because the button press was used for both types of imagery it cannot easily explain differences observed between the two. Nonetheless, we cannot rule out the possibility that such sensorimotor processes confounded both types of imagery equally. Finally, it is possible that the frequent occurrence of kinesthetic images in our sample was influenced, in part, by subjects' physical posture during falling asleep. For example, they may have been nodding or sliding slightly while falling asleep. We have, in previous studies (Nielsen, 1991, 1995), noted this type of correspondence between physical state and kinesthetic content. Indeed, subtle movements are often cited as the source of the intense 'hypnic jerks' of falling into space. The possibility of postural influences on imagery cannot be excluded on the basis of our present findings because we had no objective measures of posture or movements during the falling asleep task. Further experimental study of such factors is clearly called for.

ACKNOWLEDGMENTS

The authors wish to acknowledge the editorial help of Tyna Paquette.

REFERENCES

1. Antrobus JS. Cortical hemisphere asymmetry and sleep mentation. *Psychol Rev* 1987; 94: 359-68.
2. Baillarger M. De l'influence de l'état intermédiaire à la veille et au sommeil sur la production et la marche des hallucinations. *Annales Medico Psychologiques* 1845; 4: 168-95.
3. Bertini M, Violani C. Cerebral hemispheres, REM sleep, and dreaming. In: Bosinelli M, Cicogna P, eds. *Psychology of dreaming*. Bologna: Cooperativa Libraria Universitaria Editrice, 1984; pp. 131-6.
4. Bosinelli M, Cavallero C, Cicogna P. Self-representation in dream experiences during sleep onset and REM sleep. *Sleep* 1982; 5: 290-9.
5. Braun AR, Balkin TJ, Wesensten NJ, Carson RE, Varga M, Baldwin P, Selbie S, Belenky G, Herscovitch P. Regional cerebral blood flow throughout the sleep-wake cycle - an (H_2O)-O-15 PET study. *Brain* 1997; 120: 1173-97.
6. Cicogna P. Dreaming during sleep onset and awakening. *Perc Mot Sk* 1994; 78: 1041-2.
7. Cicogna P, Cavallero C, Bosinelli M. Cognitive aspects of mental activity during sleep. *Am J Psychol* 1991; 104: 413-25.
8. Davis H, Davis PA, Loomis AL, Harvey EN, Hobart G. Human brain potentials during the onset of sleep. *J Neurophysiol* 1938; 1: 24-38.

9. Decety J. The neurophysiological basis of motor imagery. *Beh Brain Res* 1996; 77: 45-52.
10. Dement W, Kleitman N. The relationship of eye movement during sleep to dream activity: An objective method for the study of dreaming. *J Exp Psychol* 1957; 53: 339-46.
11. Duffy FH, Bartels PH, Burchfiel JL. Significance probability mapping: An aid in the topographic analysis of brain electrical activity. *EEG Clin Neurophysiol* 1981; 51: 455-62.
12. Foulkes D, Vogel G. Mental activity at sleep onset. *J Abn Psychol* 1965; 70: 231-43.
13. Germain A, Nielsen T. Spectral analysis of global 40-Hz EEG rhythm during sleep onset imagery and wakefulness. *Sleep Res* 1996; 25: 135.
14. Green E, Green A, Walters D. Voluntary control if internal states: psychological and physiological. *J Transp Psychol* 1970; 1: 1-26.
15. Greenberg MS, Farah MJ. The laterality of dreaming. *Brain Cogn* 1986; 5: 307-21.
16. Hayashi H, Iijima S, Sugita Y, Teshima T, Tashiro T, Matsuo R, Yasoshima A, Hishikawa Y, Ishihara T. Appearance of frontal mid-line theta rhythm during sleep and its relation to mental activity. *EEG Clin Neurophysiol* 1987; 66: 66-70.
17. Hayashi M, Katoh K, Hori T. Hypnagogic imagery and EEG activity. *Perc Mot Sk* 1999; 88: 676-8.
18. Hofle N, Paus T, Reutens D, Fiset P, Gotman J, Evans AC, Jones BE. Regional cerebral blood flow changes as a function of delta and spindle activity during slow wave sleep in humans. *J Neurosci* 1997; 17: 4800-8.
19. Hori T, Hayashi M, Morikawa T. Topographical EEG changes and the hypnagogic experience. In: *Anonymous Sleep onset: Normal and abnormal processes*. Washington, DC: American Psychological Association, 1994; pp. 237-53.
20. Kuhlo W, Lehmann D. Das Einschlaferleben und seine neurophysiologischen korrelate. *Arch Psychiatr Nervenkr* 1964; 205: 687-716.
21. Lehmann D, Grass P, Meier B. Spontaneous conscious covert cognition states and brain electric spectral states in canonical correlations. *Int J Psychophysiol* 1995; 19: 41-52.
22. Lehmann D, Henggeler B, Koukkou M, Michel CM. Source localization of brain electric-field frequency bands during conscious, spontaneous visual-imagery and abstract thought. *Brain Res Cogn Brain Res* 1994; 1: 203-10.
23. Lerner B. Dream function reconsidered. *J Abn Psychol* 1967; 72: 85-100.
24. Liberson WT, Liberson CW. EEG records, reaction times, eye movements, respiration, and mental content during drowsiness. *Rec Adv Bio Psychiat* 1965; 8: 295-302.
25. Maury A. Des hallucinations hypnagogiques, ou des erreurs des sens dans l'etat intermediaire entre la veille at le sommeil. *Annales Medico-Psychologiques* 1848; 11: 26-40.
26. Merica H, Gaillard JM. The EEG of the sleep onset period in insomnia: A discriminant analysis. *Physiol Beh* 1992; 52: 199-204.
27. Michida N, Ebata A, Tanaka H, Hayashi M, Hori T. Changes of amplitude and topographical characteristics of event-related potentials during the hypnagogic period. *Psychiat Clin Neurosci* 1999; 53: 163-5.
28. Michida N, Hayashi M, Hori T. Comparison of event related potentials with and without hypnagogic imagery. P*sychiat Clin Neurosci* 1998; 52: 145-7.
29. Morikawa T, Hayashi M, Hori T. Auto power and coherence analysis of delta-theta band EEG during the waking-sleeping transition period. *EEG Clin Neurophysiol* 1997; 103: 633-41.
30. Newton PM. Recalled dream content and the maintenance of body image. *J Abn Psychol* 1970; 76: 134-9.
31. Nielsen TA. A self-observational study of spontaneous hypnagogic imagery using the upright napping procedure. *Imag Cogn Pers* 1991; 11: 353-66.
32. Nielsen TA. Describing and modeling hypnagogic imagery using a systematic self-observation procedure. *Dreaming* 1995; 5: 75-94.
33. Nielsen TA, Germain A, Ouellet L. Atonia-signalled hypnagogic imagery: Comparative EEG mapping of sleep onset transitions, REM sleep and wakefulness. *Sleep Res* 1995; 24: 133.
34. Ogilvie RD, Simons IA, Kuderian RH, MacDonald T, Rustenburg J. Behavioral, event-related potential, and EEG/FFT changes at sleep onset. *Psychophysiol* 1991; 28: 54-64.
35. Pivik RT, Broughton RJ, Coppola R, Davidson RJ, Fox N, Nuwer MR. Guidelines for the recording and quantitative analysis of electroencephalographic activity in research contexts. *Psychophysiol* 1993; 30: 547-58.
36. Richardson J, Mavromatis A, Mindel T, Owens A. Individual differences in hypnagogic and hypnopompic imagery. *J Ment Imag* 1981; 5: 91-6.
37. Solms M. *The neuropsychology of dreams*. Mahwah, New Jersey: Lawrence Erlbaum Associates, 1997.
38. Stellate Système Enr. RHYTHM 9.0. Montréal, Québec, Canada 1995.
39. Tanaka H, Hayashi M, Hori T. Statistical features of hypnagogic EEG measured by a new scoring system. *Sleep* 1996; 19: 731-8.
40. Tanaka H, Hayashi M, Hori T. Topographical characteristics and principal component structure of the hypnagogic EEG. *Sleep* 1997; 20: 523-34.
41. Tanaka H, Hayashi M, Hori T. Topographic mapping of electroencephalography coherence in hypnagogic state. *Psychiat Clin Neurosci* 1998; 52: 147-8.
42. Tanaka H, Hayashi M, Hori T. Topographical characteristics of slow wave activities during the transition from wakefulness to sleep. *Clin Neurophys* 2000; 111: 417-27.
43. Vogel G, Foulkes D, Trosman H. Ego functions and dreaming during sleep onset. *Arch Gen Psychiatr* 1966; 14: 238-48.
44. Vogel GW. Sleep-onset mentation. In: Arkin AM, Antrobus JS, Ellman SJ, eds. *The mind in Sleep*. Hillsdale: Lawrence Erlbaum Associates, 1978; pp. 97-108.
45. Wackermann J, Buechi S, Strauch I, Lehmann D. EEG correlates of altered states of consciousness at sleep onset and under reduced sensory input. *Int J Psychophysiol* 2000; 35: 40-1.